Inorg. Chem. **2006**, *45*, 7286–7294

Vacancy Ordering in $SmGe_{2-x}$ and $GdGe_{2-x}$ ($x = 0.33$): Structure and Properties of Two Sm_3Ge_5 Polymorphs and of Gd_3Ge_5

Paul H. Tobash, Daniel Lins, and Svilen Bobev*

Department of Chemistry and Biochemistry, University of Delaware, Newark, Delaware 19716

Namjung Hur, Joe D. Thompson, and John L. Sarrao

Materials Science and Technology Division, Los Alamos National Laboratory, Los Alamos, New Mexico 87545

Received May 25, 2006

The crystal structures and the magnetic properties of three new binary rare-earth intermetallic phases are reported. α-Sm_3Ge_5 and β-Sm_3Ge_5 and Gd_3Ge_5 have been prepared from the corresponding elements through high-temperature reactions using the flux-growth method. The structures of the three compounds have been established using single-crystal X-ray diffraction: α-Sm_3Ge_5 crystallizes with its own type in the hexagonal space group $P\bar{6}2c$ (No. 190) with cell parameters $a = 6.9238(11)$ Å, $c = 8.491(3)$ Å, and $Z = 2$, whereas β-Sm_3Ge_5 adopts the face-centered orthorhombic Y_3Ge_5 type with space group $Fdd2$ (No. 43) and with cell parameters $a = 5.8281(6)$ Å, $b = 17.476(2)$ Å, $c = 13.785(2)$ Å, and $Z = 8$. The orthorhombic Gd_3Ge_5 with cell parameters $a = 5.784(2)$ Å, $b = 17.355(6)$ Å, and $c = 13.785(5)$ Å is isostructural with β-Sm_3Ge_5. The structures of the title compounds can be described as AlB_2 and α-$ThSi_2$ derivatives with long-range ordering of the germanium vacancies. Temperature-dependent DC magnetization (5–300 K) measurements show evidence of antiferromagnetic ordering below ca. 30 and 10 K for α-Sm_3Ge_5 and β-Sm_3Ge_5, respectively. Gd_3Ge_5 undergoes two successive magnetic transitions below ca. 15 and 11 K. The temperature dependence of the resistivity and heat capacity of Gd_3Ge_5 are discussed as well.

Introduction

The experimental and theoretical investigation of superconductivity, especially when unconventional, that is, beyond the phonon-mediated variety explained by the Bardeen, Cooper, and Schrieffer theory,[1] has always been of fundamental importance. Of particular interest to the scientists in the field remains the connection between the dimensionality (anisotropy) of the crystal structure and the electron correlations leading to the formation of the Cooper pairs (spin-up/spin-down conduction electron pairs) that are responsible for the superconductivity, as well as the interaction between the magnetism and superconductivity, which are generally competing effects. Several important discoveries of coexisting superconductivity and ferromagnetism in $ZrZn_2$[2] and UGe_2,[3] for example, or that of the important magnetic interactions in the three-dimensional perovskite-like $MgCNi_3$ superconductor,[4] provided new outlooks which are in contrast with the conventional ideas regarding the origin of superconductivity. Another unexpected discovery, that of superconductivity in MgB_2[5] with the layered AlB_2 structure,[6] challenged the widely accepted view that noncubic and transition-metal free intermetallic compounds cannot be superconductors above 30 K. These recent advances suggest that fundamental concepts pertaining to the magnetic order–disorder phenomena and superconductivity need to be re-evaluated.

* Author to whom correspondence should be addressed. Phone: (302) 831-8720. Fax: (302) 831-6335. E-mail: sbobev@chem.udel.edu.

(1) Bardeen, J.; Cooper, L. N.; Schriefer, J. R. *Phys. Rev.* **1957**, *106*, 162.
(2) Pfleiderer, C.; Uhlarz, M.; Hayden, S. M.; Vollmer, R.; Löhneysen, H. v.; Bernhoeft, N. R.; Lonzarich, G. G. *Nature* **2001**, *412*, 58.
(3) Saxena, S. S.; Agarwal, P.; Ahilan, K.; Grosche, F. M.; Haselwimmer, R. K. W.; Steiner, M. J.; Pugh, E.; Walker, I. R.; Julina, S. R.; Monthoux, P.; Lonzarich, G. G.; Huxley, A.; Sheikin, I.; Braithwaite, D.; Flouquet, J. *Nature* **2000**, *406*, 587.
(4) He, T.; Huang, Q.; Ramirez, A. P.; Wang, Y.; Regan, K. A.; Rogado, N.; Hayward, M. A.; Haas, M. K.; Slusku, J. S.; Inumara, K.; Zandbergen, H. W.; Ong, N. P.; Cava, R. J. *Nature* **2001**, *411*, 54.
(5) Nagamatsu, J.; Nakagawa, N.; Muranaka, T.; Zenitani, Y.; Akimitsu, J. *Nature* **2001**, *410*, 6824.
(6) Villars, P.; Calvert, L. D. *Pearson's Handbook of Crystallographic Data for Intermetallic Phases*, 2nd ed.; American Society for Metals: Materials Park, OH, 1991.

10.1021/ic060913f CCC: $33.50
Published on Web 07/28/2006

Intrigued by the opportunity to deepen the understanding of how the local order of magnetic moments may give rise to unique properties in various classes of polar intermetallic compounds (i.e., intermetallic compounds, in which one of the components is far less electronegative than the other), we undertook systematic exploratory studies in the germanium-rich part of the RE−Ge systems (RE = *r*are-*e*arth). This choice was not accidental—these are materials with diverse structures, many of which are structurally related to MgB_2, and thus have attracted much attention in recent years.[7−12] However, their electronic and transport properties are still not well-understood because of the subtle effects traditional solid-state syntheses and impurity levels play on their physical properties.[13] This is particularly true for the $REGe_2$ compounds, where the ideal "1−2" composition is rarely realized and various $REGe_{2-x}$ ($0 < x < 0.5$) substoichiometric compounds abound.[14]

Motivated by the successful application of the flux-growth methods in our previous studies,[15] it was anticipated that using low-melting indium metal, for instance, could facilitate the nucleation and the crystal growth of such phases, and they could be readily synthesized and their structures and properties could be established reliably. The synthetic efforts using In flux, so far, have shown that the mid-to-late lanthanides do react with In and Ge to form ternary RE_2InGe_2 phases (RE = Sm, Gd−Ho, and Yb).[15] In the Sm−In−Ge system, in addition to the novel ternary Sm_2InGe_2 compound, the use of In as a metal flux afforded the formation of two new binary compounds, both with composition Sm_3Ge_5 but with two different structures—one crystallizing with a new hexagonal type [space group $P\bar{6}2c$ (No. 190), Pearson's symbol hP16] and another one of the orthorhombic Y_3Ge_5 type,[6] [space group *Fdd*2 (No. 43), Pearson's symbol oF64]. The structures of both polymorphs (hereafter, denoted as α-Sm_3Ge_5 and β-Sm_3Ge_5, for the hexagonal and the orthorhombic forms, respectively) can be derived from the ubiquitous AlB_2 and α-$ThSi_2$ types through long-range ordering of Ge vacancies. Herein, we report comprehensive single-crystal and powder X-ray diffraction studies and temperature-dependent DC magnetization measurements of both Sm_3Ge_5 polymorphs and of Gd_3Ge_5, which is isostructural with β-Sm_3Ge_5. Reported as well are the electrical resistivity and the heat capacity of Gd_3Ge_5. A short analysis of the bonding, the relative stability of the α- and β-Sm_3Ge_5 forms, and the structural trends across the series are also discussed.

Experimental Section

Synthesis. All manipulations were performed inside an argon-filled glovebox with controlled oxygen and moisture levels below 1 ppm or under a vacuum. The starting materials—Sm (pieces, >99.9%, Ames Laboratory), Ge (lump, 99.999%, Acros), and In (shot, 99.99%, Alfa-Aesar)—were used as received. The reactions were carried out in alumina crucibles (Coors, 2 cm^3), which were subsequently enclosed in fused silica ampules and flamed-sealed under a vacuum. In the original experiment, a reaction mixture containing the starting materials in a ratio of Sm/Ge/In = 1:1:10 was heated quickly (rate ca. 300°/h) to 1373 K, allowed to equilibrate at this temperature for 1.5 h, and then cooled to 673 K over a period of 20 h. At this point, the reaction was taken out from the furnace and the excess indium metal (mp 430 K) was removed by centrifugation. Further and more elaborate details on the flux-growth procedure can be found elsewhere.[15] The reaction outcome consisted of a mixture of crystals with different morphologies: needles of the Sm_2InGe_2 compound,[15] irregular pieces of α-Sm_3Ge_5, and small cube-shaped crystals of $SmIn_3$.[6]

In subsequent reactions aimed at forming α-Sm_3Ge_5 in a larger yield, the elements were loaded with Sm/Ge ratios from 1:1 to 1:1.5 and a 10- to 20-fold excess of In. Various temperature profiles were explored, which included both quick and slow ramping of the temperature to 1273 or 1373 K, equilibration from 1 to 24 h, and a variety of cooling steps. In all instances, the reactions produced multiple phases, and no conditions for growing large single crystals of α-Sm_3Ge_5 were found. However, during the course of these experiments, a new orthorhombic polymorph (β-Sm_3Ge_5) was discovered.

β-Sm_3Ge_5 forms exclusively from reactions of the elements loaded with the Sm/Ge ratio of 1:1.5 and a 10-fold excess of In that were quickly heated to 1273 K, held for 1.5 h, and then slowly (ca. 10°/h) cooled to 773 K. This means that reactions, which nominally produce the hexagonal polymorph could also produce the orthorhombic modification if allowed to cool at a slower rate. It was also discovered that reactions which were heated for 24−72 h at intermediate temperatures, 1073 K, for instance, produce plate-like crystals of β-Sm_3Ge_5 as a sole product.

The synthesis of Gd_3Ge_5 was carried out in a similar way using In flux as a growth medium. In these reactions, the outcome was found to be strongly dependent on the nominal composition and not so much on the temperature profile—under the same conditions, a reaction mixture containing Gd and Ge in a ratio of 1:1 and a 10-fold excess of In yields quantitatively Gd_2InGe_2,[15] whereas the reaction mixture containing Gd and Ge in a ratio of 1:1.5 and a 10-fold excess of In yields Gd_3Ge_5. In these syntheses, just like with the Sm reactions, a slight excess of rare-earth metal is needed to compensate for the metal, which is invariably lost because of secondary reactions with the flux to form $GdIn_3$ or $SmIn_3$ binaries.[6] Attempts to prepare Gd_3Ge_5 isostructural to α-Sm_3Ge_5 have been unsuccessful so far. Syntheses of different rare-earth analogues of the "3−5" family using In and other metal fluxes were also attempted; however, these reactions produced assorted $REGe_{2-x}$ ($0.25 < x < 0.4$) compounds, and the results of these studies will be published in forthcoming publications.

(7) Mozharivskyj, Y.; Pecharsky, A. O.; Pecharsky, V. K.; Miller, G. J. *J. Am. Chem. Soc.* **2005**, *127*, 317.
(8) Choe, W.; Pecharsky, A. O.; Wörle, M.; Miller, G. J. *Inorg. Chem.* **2003**, *42*, 8223.
(9) Mozharivskyj, Y.; Choe, W.; Pecharsky, A. O.; Miller, G. J. *J. Am. Chem. Soc.* **2003**, *125*, 15183.
(10) Mao, J.-G.; Goodey, J.; Guloy, A. M. *Inorg. Chem.* **2002**, *41*, 931.
(11) Ahn, K.; Tsokol, A. O.; Mozharivskyj, Y.; Gschneidner, K. A., Jr.; Pecharsky, V. K. *Phys. Rev. B: Condens. Matter Mater. Phys.* **2005**, *72*, 054404.
(12) Levin, E. M.; Pecharsky, V. K.; Gschneidner, K. A., Jr.; Miller, G. J. *Phys. Rev. B: Condens. Matter Mater. Phys.* **2001**, *64*, 235103.
(13) Because of the synthetic difficulties associated with the synthesis and characterization of many rare-earth digermanides, there are numerous controversies surrounding their properties, $CeGe_2$ (or rather $CeGe_{1.66}$) being just one recent example: (a) Lin, C. L.; Yuen, T.; Riseborough, P.; Huang, X.-Y.; Li, J. *J. Appl. Phys.* **2002**, *91*, 8117. (b) Nakano, T.; Hedo, M.; Uwatoko, Y. *Physica B* **2005**, *359−361*, 284.
(14) (a) Guloy, A. M.; Corbett, J. D. *Inorg. Chem.* **1991**, *30*, 4789. (b) Venturini, G.; Ijjaali, I.; Malaman, B. *J. Alloys Compd.* **1999**, *284*, 262. (c) Venturini, G.; Ijjaali, I.; Malaman, B. *J. Alloys Compd.* **1999**, *285*, 194.
(15) Tobash, P. H.; Lins, D.; Bobev, S.; Lima, A.; Hundley, M. F.; Thompson, J. D.; Sarrao, J. L. *Chem. Mater.* **2005**, *17*, 5567.

Table 1. Selected Crystal Data and Structure Refinement Parameters for the Two Sm_3Ge_5 Polymorphs and Gd_3Ge_5

empirical formula	Sm_3Ge_5	Sm_3Ge_5	Gd_3Ge_5
fw	814.03 g/mol	814.03 g/mol	834.70 g/mol
data collection temperature	120(2) K	120(2) K	120(2) K
radiation, wavelength (λ)	Mo Kα, 0.710 73 Å	Mo Kα, 0.710 73 Å	Mo Kα, 0.710 73 Å
cryst syst	hexagonal	orthorhombic	orthorhombic
space group	$P\bar{6}2c$ (No. 190)	$Fdd2$ (No. 43)	$Fdd2$ (No. 43)
unit cell dimensions	$a = 6.9238(11)$ Å	$a = 5.8281(6)$ Å	$a = 5.784(2)$ Å
		$b = 17.476(2)$ Å	$b = 17.355(6)$ Å
	$c = 8.491(3)$ Å	$c = 13.7849(15)$ Å	$c = 13.785(5)$ Å
unit cell volume, Z	352.52(14) Å^3, 2	1413.2(3) Å^3, 8	1383.8(8) Å^3, 8
density (ρ_{calc})	7.669 g/cm^3	7.652 g/cm^3	8.013 g/cm^3
abs coeff (μ)	45.444 mm^{-1}	45.344 mm^{-1}	49.601 mm^{-1}
final R indices[a] [$I > 2\sigma_{(I)}$]	$R_1 = 0.0162$	$R_1 = 0.0198$	$R_1 = 0.0193$
	$wR_2 = 0.0366$	$wR_2 = 0.0479$	$wR_2 = 0.0465$
final R indices[a] [all data]	$R_1 = 0.0215$	$R_1 = 0.0201$	$R_1 = 0.0200$
	$wR_2 = 0.0382$	$wR_2 = 0.0480$	$wR_2 = 0.0470$

[a] $R_1 = \sum||F_o| - |F_c||/\sum|F_o|$, $wR_2 = [\sum[w(F_o^2 - F_c^2)^2]/\sum[w(F_o^2)^2]]^{1/2}$, $w = 1/[\sigma^2F_o^2 + (AP)^2 + BP]$, and $P = (F_o^2 + 2F_c^2)/3$; A and B are weight coefficients.

The In flux-grown crystals of Gd_3Ge_5 and of both polymorphs of Sm_3Ge_5 exhibit a silver-metallic luster and appear air- and moisture-stable over periods of time greater than 12 months.

Powder X-ray Diffraction. X-ray powder diffraction patterns were taken at room temperature on a Rigaku MiniFlex powder diffractometer using monochromatized Cu Kα radiation. Typical runs included $\theta-\theta$ scans ($2\theta_{max} = 90°$) with intervals of 0.02° and a 10 s counting time. The data analysis was carried out using the JADE 6.5 software package.[16] Samples were prepared by grinding flux-grown crystals to fine powder. The intensities and the positions of the experimentally observed peaks matched very well with those calculated from the crystal structures.

Single-Crystal X-ray Diffraction. Crystals for data collection were chosen from different reactions and cut in Paratone N oil to suitable dimensions (ca. 0.05 mm in all dimensions) and then mounted on glass fibers. For all three compounds, full spheres of single-crystal X-ray diffraction data were collected at 120 K on a Bruker SMART CCD-based diffractometer. The data collections were handled routinely in batch runs at different ω and ϕ angles. The frame width was 0.4° or 0.5° in ω and θ with a data acquisition time of 10 s/frame. The data collection, data integration, and cell refinement were done using the SMART and SAINT programs.[17]. SADABS[18] was used for semiempirical absorption correction based on equivalents. The structures were solved by direct methods and refined by full-matrix least-squares methods on F^2 using the SHELX package.[19] Further details of the data collection and structure refinement parameters are given in Table 1.

In the last refinement cycles, the atomic positions for the α-Sm_3Ge_5 polymorph were standardized using STRUCTURE TIDY,[20] and all sites were refined with anisotropic displacement parameters. For the orthorhombic structures of Sm_3Ge_5 and Gd_3Ge_5, the labeling scheme and atomic positions from the previously reported RE_3Ge_5 (RE = Nd, Tb, Dy, and Ho)[21] were used for uniformity. Final positional and equivalent isotropic displacement parameters and important bond distances are listed in Tables 2 and 3, respectively. The crystallographic information files (CIF) have also been deposited with Fachinformationszentrum Karlsruhe [76344 Eggenstein-Leopoldshafen, Germany; fax: (49) 7247-808-666; e-mail: crysdata@fiz.karlsruhe.de; depository numbers CSD-416581 (α-Sm_3Ge_5), CSD-416582 (β-Sm_3Ge_5), and CSD-416583 (Gd_3Ge_5)].

It needs to be pointed out here that, because both structures are ordered variants of the ubiquitous AlB_2 and α-$ThSi_2$ types,[6]

Table 2. Atomic Coordinates and Equivalent Isotropic Displacement Parameters (U_{eq}[a]) for the Two Sm_3Ge_5 Polymorphs[b]

atom	Wyckoff position	x	y	z	U_{eq} (Å^2)
		Hexagonal α-Sm_3Ge_5			
Sm1	6g	0.331 30(9)	0	0	0.0077(2)
Ge1	6h	0.3946(2)	0.3318(2)	1/4	0.0099(3)
Ge2	2d	1/3	2/3	1/4	0.0098(5)
Ge3	2b	0	0	1/4	0.0105(5)
		Orthorhombic β-Sm_3Ge_5			
Sm1	8a	0	0	0.000 01(5)	0.0099(2)
Sm2	16b	0.757 33(8)	0.081 69(3)	0.256 33(4)	0.0099(2)
Ge1	8a	0	0	0.4461(1)	0.0113(3)
Ge2	16b	0.7949(2)	0.069 64(6)	0.6575(1)	0.0108(2)
Ge3	16b	0.7407(1)	0.087 05(5)	0.8368(1)	0.0109(3)

[a] U_{eq} is defined as one-third of the trace of the orthogonalized U^{ij} tensor. [b] The atomic coordinates for Gd_3Ge_5 are very similar to those for the orthorhombic Sm_3Ge_5 and are given as Supporting Information.

Table 3. Selected Bond Distances in the Two Sm_3Ge_5 Polymorphs[a]

atom pair		distance (Å)	atom pair		distance (Å)
	Hexagonal α-Sm_3Ge_5			Orthorhombic β-Sm_3Ge_5	
Ge1−	Ge3	2.543(1)	Ge1−	Ge2 × 2	2.566(1)
	Ge2	2.557(2)	Ge2−	Ge1	2.566(1)
	Sm × 2	2.995(1)		Ge3	2.527(2)
	Sm × 2	3.021(1)		Ge3	2.601(1)
	Sm × 2	3.459(1)	Ge3−	Ge2	2.527(2)
Ge2−	Ge1 × 3	2.557(2)		Ge2	2.601(1)
	Sm × 6	3.1409(6)	Sm1−	Ge1 × 2	3.0083(7)
Ge3−	Ge1 × 3	2.543(1)		Ge3 × 2	3.035(2)
	Sm × 6	3.1254(7)		Ge2 × 2	3.093(1)
Sm−	Ge1 × 2	2.995(1)		Ge2 × 2	3.118(2)
	Ge1 × 2	3.021(1)		Ge3 × 2	3.413(1)
	Ge3 × 2	3.1254(7)	Sm2−	Ge3	2.983(1)
	Ge2 × 2	3.1409(6)		Ge3	2.995(1)
	Ge1 × 2	3.459(1)		Ge3	3.031(1)
				Ge2	3.012(1)
				Ge1	3.0579(9)
				Ge2	3.066(2)
				Ge2	3.153(1)
				Ge2	3.213(1)
				Ge1	3.313(2)
				Ge3	3.427(1)

[a] The distances in Gd_3Ge_5 are very similar to those for the orthorhombic Sm_3Ge_5 and are provided as Supporting Information.

(16) *JADE*, version 6.5; Materials Data, Inc.: Livermore, CA, 2003.
(17) (a) *SMART NT*, version 5.63; Bruker Analytical X-ray Systems, Inc.: Madison, WI, 2003. (b) *SAINT NT*, version 6.45; Bruker Analytical X-ray Systems, Inc.: Madison, WI, 2003.
(18) *SADABS NT*, version 2.10; Bruker Analytical X-ray Systems, Inc.: Madison, WI, 2001.
(19) (a) *SHELXS-97*; Bruker Analytical Systems, Inc.: Madison, WI, 1990. (b) *SHELXTL*, version 6.12; Bruker Analytical X-ray Systems, Inc.: Madison, WI, 2001.
(20) Gelato, L. M.; Parthe, E. *J. Appl. Crystallogr.* **1987**, *20*, 139.

additional refinements were carried out using the latter as models. For that purpose, the intensity data were reintegrated using orientation matrixes obtained from the subcells—hexagonal with $a = 3.990(1)$ Å and $c = 4.237(2)$ Å for α-Sm_3Ge_5 and body-centered tetragonal with $a = 4.0931(9)$ Å and $c = 13.799(6)$ Å for Gd_3Ge_5 (Supporting Information). The initial refinement cycles with isotropic thermal parameters confirmed the validity of the model and converged to R_1 values around 12−15%. In the next refinement cycles, the Ge atoms were refined with freed occupation factors, which resulted in formula units $SmGe_{2-x}$ and $GdGe_{2-x}$ with x being close to $^1/_3$. The overall refinement improved, yet the final residuals were on the high side for such small structures. During the subsequent structure refinements with anisotropic thermal parameters, however, a problem with the temperature parameters for the Ge atoms became apparent—they were abnormally elongated in certain ways in both cases. All of the above, together with the powder diffraction data, which also show some of the stronger superstructure reflections, suggested that superstructures with unit cells that are 6 times larger than those of the parent compounds account for the long-range order of the Ge vacancies in both Sm_3Ge_5 polymorphs and in Gd_3Ge_5. A detailed discussion and tables with crystallographic data from the subcell refinements are provided as Supporting Information.

Magnetic Susceptibility Measurements. Field-cooled and zero-field-cooled dc magnetization (M) measurements were performed for single crystals of the title compounds using a Quantum Design MPMS SQUID magnetometer. The measurements were completed in the temperature range from 5 to 300 K and in an applied magnetic field (H) of 500 Oe. The samples were secured in a custom-designed low-background sample holder. The raw magnetization data were collected for the holder contribution and converted to molar susceptibility. All of the crystals measured were carefully selected from the reaction products, and the phase purity was assessed from the corresponding powder X-ray diffraction patterns.

Specific Heat and Resistivity Measurements. The electrical resistivity and the heat capacity were measured in a Quantum Design PPMS system. Multiple measurements on different specimens were carried out to ensure reproducibility. The resistance was measured using the four-probe technique from 2 to 300 K with an excitation current of 1 mA. The ohmic contacts to the polished surface of the chosen single crystals were made by spot welding. Calorimetry data for the same specimens were taken using the thermal relaxation method. Only measurements for flux-grown single crystals of Gd_3Ge_5 are reported herein; the crystals of either α-Sm_3Ge_5 or β-Sm_3Ge_5 were too small to warrant trouble-free contacts and to minimize the geometric errors.

Results and Discussion

Synthesis, Structure, and Bonding. The hexagonal α-Sm_3Ge_5 polymorph crystallizes in a new crystal structure with its own type (Pearson's code hP16) in the noncentrosymmetric space group $P\bar{6}2c$ (No. 190), and a schematic representation of the structure is shown in Figure 1. The structure is best described as an alternate stacking of defect graphite-like layers of germanium with samarium cations sandwiched between them. This structure is most conveniently derived from the parent $SmGe_{2-x}$ structure (AlB_2 type, space group $P6/mmm$, and $a \approx 4.0$ and $c \approx 4.2$ Å) through ordering of the Ge vacancies. Using this approach, the removal of every sixth Ge atom from the hexagonal layer in a regular fashion, concomitant small distortion as shown in Figure 2, will result in a long-range vacancy order in the ab plane. The result is a net of fused 12-membered rings, which are analogous to those of [12]-annulene. If the hexagonal symmetry is preserved, the new crystallographic unit cell will have a cell parameter $a' \approx a \times 3^{1/2}$ (Figure 2); in the other most-likely scenario, where the high rotational symmetry is lost, the result will be an ortho-hexagonal (or monoclinic) cell with $a' \approx a \times 3^{1/2}$ and $b' \approx b$. In the event that the layers continue to be flat and the stacking sequence of the layers remains the same as in the parent AlB_2 type (eclipsed, on top of each other), the c axis will not change. If the layers with ordered vacancies become slightly puckered or the stacking sequence changes, the c axis is expected to double (just like in α-Sm_3Ge_5) or triple. Other structural models using this rationale have been proposed as well, and the corresponding crystallographic group−subgroup relationships according to the Bärnighausen formalism have already been worked out.[22] Nonetheless, most rare-earth digermanides with the AlB_2 type are known to be nonstoichiometric,[14] yet the vast majority of the reports on their structures and properties assume an entirely statistical distribution of the Ge vacancies. There are only a few structures with full long-range vacancy ordering as described

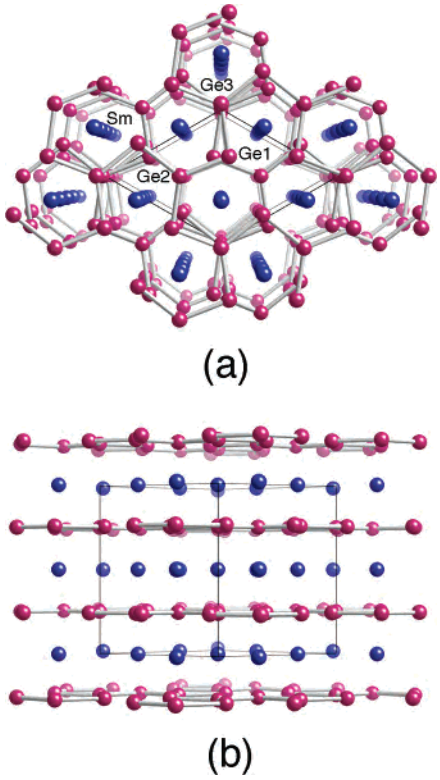

Figure 1. Perspective view of the hexagonal structure of α-Sm_3Ge_5, viewed down the c axis (a) and down the [110] direction (b). Sm atoms are shown as dark-blue spheres, and the Ge atoms are drawn as maroon spheres. The unit cell is outlined.

(21) (a) Schobinger-Papamantellos, P.; Buschow, K. H. J. *J. Magn. Magn. Mater.* **1989**, *82*, 99. (b) Schobinger-Papamantellos, P.; Buschow, K. H. J. *J. Less-Common Met.* **1989**, *146*, 279. (c) Schobinger-Papamantellos, P.; de Mooij, D. B.; Buschow, K. H. J. *J. Less-Common Met.* **1990**, *163*, 319. (d) Zaharko, O.; Schobinger-Papamantellos, P.; Ritter, C. *J. Alloys Compd.* **1998**, *280*, 4.

(22) Hoffman, R.-D.; Pöttgen, R. *Z. Kristallogr.* **2001**, *216*, 127.

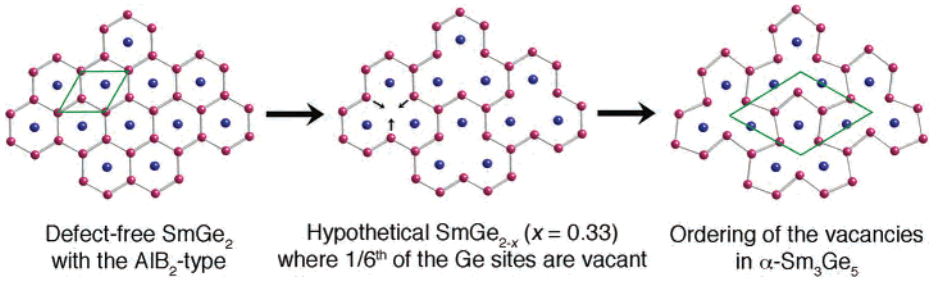

Figure 2. Schematic representation of the process of creating long-range vacancy order in the graphitelike layers of Ge and with the corresponding unit cell. Color code as in Figure 1.

above—Yb_3Ge_5 with the Th_3Pd_5 type (Pearson's hP8, space group $P\bar{6}2m$, 3 times the volume of the basic subcell) being just one well-known example.[23] Analogously, $RE_{15}Ge_9Z$ (Z = transition metal, C, O, and P) interstitial derivatives of RE_5Ge_3 are known to crystallize with an ordered superstructure of their parent Mn_5Si_3 type.[24]

Structure refinements of α-Sm_3Ge_5 using the parent AlB_2 structure as a model provide several key indicators that point to the possibility for full vacancy ordering (see the Supporting Information). Among these, the abnormal elongation of the Ge anisotropic displacement parameter in the *ab* plane and the unusually short Ge−Ge contacts are worth special attention. The refined Ge−Ge distances of ca. 2.3 Å are 7−8% shorter than the Ge−Ge contacts in elemental Ge (diamond-type structure).[25] These distances are exceptionally short for such a solid-state structure, and the presumption of nonclassical bonding ought to be used in order to rationalize such connectivity and network topology.[26] However, the vacancy-ordering scheme and the displacement of the Ge1 atom (Table 2 and Figure 2) toward the created empty space allows for the "relaxation" of the strained bonds. This distortion of the defect honeycomb layer is significant: Ge1 is moved 0.430(2) Å away in a direction toward the vacancy, and the corresponding Ge−Ge−Ge angles are 103.22(5)° rather than 120°. Hence, the refined Ge−Ge distances in α-Sm_3Ge_5 using the superstructure model become "normal"—ranging from 2.543(1) to 2.557(2) Å (Table 3). The values are slightly longer than the Ge−Ge distances in elemental Ge but compare well with the ones reported for other rare-earth or alkaline-earth germanides with ordered structures, where the germaniums are in partially reduced oxidation states.[7−12,15,21,27]

The long-range ordering of the defects has an implication over the Sm coordination polyhedron and the crystal field splitting of the corresponding f states. Each samarium cation is now coordinated by 10 next-nearest Ge neighbors with distances falling in the range 2.995(1)−3.459(1) Å (Table 3). The shape of the polyhedron resembles more that of a

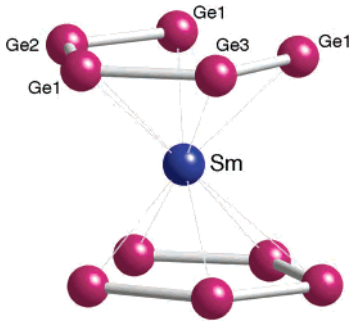

Figure 3. Coordination polyhedron around the Sm atoms in the structure of α-Sm_3Ge_5. The corresponding bond distances are listed in Table 3.

distorted pentagonal antiprism (ferrocene-like) as shown in Figure 3, rather than a regular 12-vertex polyhedron with the shape of a hexagonal prism as in the parent AlB_2 type.[6,22] The Ge subnetwork distortions have no effect on the closest Sm−Sm contacts [3.973(1) Å] because the Sm atoms are in special positions (Table 2). Nevertheless, the changes in the local coordination may have a major effect on the ground 4f *J* multiplets that account for the magnetic properties. This might be particularly important for the Sm^{3+} cation, which carries a unique magnetic moment as its spin and orbital moments are coupled strongly by spin−orbit interaction so that they almost cancel out. Obviously, these subtle changes in the energy splitting due to the crystal field effect need to be taken into consideration when explaining the magnetic moment interactions in such compounds.

The structures of β-Sm_3Ge_5 and of Gd_3Ge_5 (Figure 4) belong to the face-centered orthorhombic Y_3Ge_5 type (Pearson's code oF64) and can be derived from the parent α-$ThSi_2$ type (space group $I4_1/amd$),[6] again through the ordering of Ge vacancies. Besides the archetype, there are several other members of this family whose structures and properties have already been reported—Nd_3Ge_5, Tb_3Ge_5, Dy_3Ge_5, and Ho_3Ge_5.[21] Because many crystallographic details of this structure type have been given elsewhere,[21] only a concise description in the context of this work will be provided herein.

β-Sm_3Ge_5 and Gd_3Ge_5 feature three-dimensional frameworks of Ge atoms with rare-earth cations occupying the channels created within them (Figure 4). The framework topology can be derived from the interpenetration of two perpendicular graphite-like sheets, or alternatively, it can be viewed as infinite polyene-like chains of germanium atoms running along two directions.[14,21,26] Using the approach described above for the hexagonal α-Sm_3Ge_5, the structure of the β form can also be derived from that of the parent

(23) Grytsiv, A.; Kaczorowski, D.; Leithe-Jasper, A.; Rogl, P.; Potel, M.; Noël, H.; Pikul, A. P.; Velikanova, T. *J. Solid State Chem.* **2002**, *165*, 178.
(24) Guloy, A. M.; Corbett, J. D. *Inorg. Chem.* **1996**, *35*, 4669.
(25) Pauling, L. *The Nature of the Chemical Bond*; Cornell University Press: Ithaca, NY, 1960.
(26) Hoffmann, R.; Hughbanks, T.; Kertész, M. *J. Am. Chem. Soc.* **1983**, *105*, 4831.
(27) (a) Bobev, S.; Bauer, E. D.; Thompson, J. D.; Sarrao, J. L.; Miller, G. J.; Eck, B.; Dronskowski, R. *J. Solid State Chem.* **2004**, *177*, 3545. (b) Tobash, P. H.; Bobev, S. *J. Am. Chem. Soc.* **2006**, *128*, 3532.

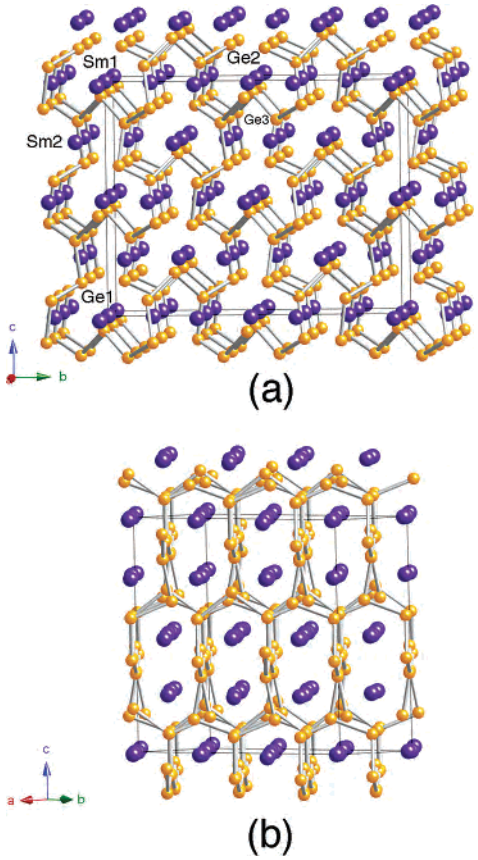

Figure 4. Perspective view of the orthorhombic structure of β-Sm_3Ge_5, viewed down the *a* axis (a) and in the direction almost parallel to the [130] plane (b). Sm atoms are shown as purple spheres, and the Ge atoms are drawn as golden spheres. The unit cell is outlined.

$SmGe_{2-x}$ and $GdGe_{2-x}$ compounds (space groups $I4_1/amd$ or *Imma*) by the removal of every sixth Ge atom in a regular fashion. This allows for the complete order of the vacant sites, and the "defect" Ge network distorts significantly to compensate for the created empty spaces, just like in α-Sm_3Ge_5 (Figure 2). Importantly, such distortion provides the mechanism for the Ge atoms to move away from one another; otherwise, the Ge−Ge distances would have been unrealistically short (Supporting Information). Such a problem hinders severely the rationalization of the bonding in these and related compounds because it will require multiple bonding as was previously discussed, yet the π clouds of neighboring chains will be too close to account for this hypothetical conjugation.[26] Apparently, most of if not all of the substoichiometric rare-earth digermanides with the α-$ThSi_2$ type necessitate some structure distortion to relieve this "strain", and the orthorhombic deformation discussed herein is one possible way of doing it—Tables 2 and 3 list the positional and thermal displacement parameters and important bond distances, respectively.

In the β-Sm_3Ge_5 structure, the Ge−Ge interatomic distances fall in the range from 2.527(2) to 2.601(1) Å [from 2.537(2) to 2.607(2) Å in Gd_3Ge_5], and they compare well with those reported for the isostructural RE_3Ge_5 (RE = Y, Nd, and Tb−Ho) phases.[6,21] A comparison of the Ge−Ge distances among the known members of the family does not provide evidence for systematic variation or correlation with the decreasing of the unit cell volume when moving across the series.

In-depth analyses of the bonding interactions in various AlB_2 and α-$ThSi_2$ intermetallics have been given elsewhere,[22,28,29] and the effects of the vacancies and the concomitant lattice distortions have already received thorough consideration. The possibility for π conjugation in simple binary and in some more complex ternary phases as well as the importance of the cation−anion interactions have also been discussed.[26] If the possible covalent character of any Sm−Ge and Gd−Ge interactions in the title compounds is neglected (although some Sm−Ge and Gd−Ge values on the order of ca. 3 Å suggest otherwise), basic structure rationalization can be conveniently approached from a point of view of the classic Zintl formalism.[30] It can provide an overly simplistic yet not unrealistic electron count—because Ge with three covalent bond needs one extra electron to complete its valence shell, the formal oxidation state for Ge in that structure would be "1−", whereas Ge with two covalent bonds needs two extra electrons to complete its valence shell, and the formal oxidation state for Ge in that structure would be "2−". Following this formalism, the structures of α-Sm_3Ge_5, β-Sm_3Ge_5, and Gd_3Ge_5 can be rationalized as $(RE^{3+})_3(Ge^{2-})_3(Ge^{1-})_2(e^-)$, that is, metals with one electron per formula unit in the conduction band. Indeed, the temperature dependence of the resistivity for Gd_3Ge_5 shows typical metallic behavior with a room temperature value that is an order of magnitude higher than the resistivities of the noble metals (below). In other systems, such as the structurally related Yb_3Ge_5, mixed-valent behavior is reported.[23] In that case, the matrix effect on the larger Yb^{2+} cation (note that the trivalent [Xe]f^{13} and the divalent [Xe]-f^{14} configurations of Yb are very close in energy) competes with the electronic requirement of the Ge subnetwork, thereby leading to intermediate valence.[23] Thus, small changes in the crystallographic and electronic environment of the Yb cations, like doping or substitution, have a remarkable effect on the physical properties, and interesting physics could result as recently shown by us with the example of Yb_4MgGe_4.[27b]

Last, it is worthwhile to discuss the long-range vacancy ordering in the RE_3Ge_5 compounds and the existence of the two polymorphs of Sm_3Ge_5 in a wider context. After all, an inspection of the Sm−Ge binary phase diagram offers clues only for the existence of a metastable, hitherto unknown compound with a composition of $SmGe_{1.63}$, but there is no indication for the possible existence of another, high-temperature polymorph.[31] Also, as discussed already, there

(28) (a) Burdett, J. K.; Miller, G. J. *Chem. Mater.* **1990**, *2*, 12. (b) Burdett, J. K.; Canadell, E.; Miller, G. J. *J. Am. Chem. Soc.* **1986**, *108*, 6561. (c) Koch, E. *Z. Kristallogr.* **1985**, *173*, 205.
(29) (a) Zheng, C.; Hoffmann, R. *Inorg. Chem.* **1989**, *28*, 1074. (b) Lupu, C.; Downie, C.; Guloy, A. M.; Albright, T. A.; Mao, J.-G. *J. Am. Chem. Soc.* **2004**, *126*, 4386.
(30) (a) Zintl, E. *Angew. Chem.* **1939**, *52*, 1. (b) Kauzlarich, S. M. *Chemistry, Structure and Bonding of Zintl Phases and Ions*; VCH Publishers: New York, 1996; and the references therein.
(31) Massalski, T. B. *Binary Alloy Phase Diagrams*; American Society for Metals: Materials Park, OH, 1990.

are several known RE_3Ge_5 compounds (RE = Y, Nd, and Tb−Ho) with the orthorhombic Y_3Ge_5 type;[6,21] however, α-Sm_3Ge_5 represents a new type.[32]

Many of the previously reported $REGe_{2-x}$ phases have been prepared using arc-melting and annealing, and their structures have been established from their corresponding X-ray powder patterns.[13,14,21] Our approach using an excess of In metal as a medium for facile crystal growth provides an alternative route for the synthesis of these compounds. The size of the crystals, the yields, and the present side products (most commonly cubic $REIn_3$ phases) vary significantly for different rare-earths and, of course, were largely dependent on the heating/cooling profiles. In the systems La through Nd, for instance, regardless of all efforts, RE_3Ge_5 compounds could not be synthesized from In flux, although Nd_3Ge_5 has been reported and made using a different synthetic route.[21a] The major products of these reactions are new binary phases whose structures again are derivatives of the α-$ThSi_2$ type. RE_3Ge_5 compounds for RE = Eu, Er, Tm, and Lu also could not be prepared, whereas Yb_3Ge_5,[23] as already mentioned, is known and crystallizes with the Th_3Pd_5 type,[6] a structure closely related to that of α-Sm_3Ge_5. Apparently, the orthorhombic "3−5 family" extends from Nd to Ho (note that the ionic radius of Y^{3+} is almost identical to that of Ho^{3+}),[25] excluding Eu, which exists in the 2+ oxidation state in most cases. All of the above suggests that the "templating effect", that is, the size of the rare-earth cations, not the melting point or the electronic states, plays a critical role. Similar trends have been observed for the series RE_2InGe_2 (RE = Sm, Gd−Ho, and Yb).[15]

α-Sm_3Ge_5, so far, is the sole example of the new AlB_2-type superstructure, despite all attempts to synthesize other homologues.[32] The numerous reactions carried out in the Sm−In−Ge system provided firm evidence that, under fast cooling conditions, the final product is always α-Sm_3Ge_5 with trace amounts of β-Sm_3Ge_5, while slow cooling rates exclusively yield the β polymorph. If one assumes that the crystal nucleation and growth are under kinetic control, the former temperature profile will allow for the synthesis of the less stable but faster growing nuclei (i.e., α-Sm_3Ge_5); on the other hand, slow cooling or prolonged heating at intermediate temperatures will result in a transformation to the thermodynamically more stable phase (i.e., β-Sm_3Ge_5). This indicates that α-Sm_3Ge_5 is the high-temperature, metastable polymorph, while β-Sm_3Ge_5 is the thermodynamically stable, low-temperature phase. Similar polymorphism is reported for Y_3Ge_5,[32] and for $RENiGe_2$.[33] In both cases, the metastable forms can be synthesized from flux only; the thermodynamically more stable polymorphs on the other hand are accessible by standard high-temperature synthesis.

Properties. Temperature-dependent dc magnetization measurements were performed within the interval 5−300 K, and the resulting plots of the magnetic susceptibility $\chi = M/H$ versus temperature T are shown in Figure 5. Because of the small effective moment on Sm^{3+} and the significant diamagnetic core and strong van Vleck paramagnetic contributions to the magnetization, both α-Sm_3Ge_5 and β-Sm_3Ge_5 do not exhibit simple magnetic behavior comparable to Gd_3Ge_5 and the other localized f-electron systems. Therefore, the magnetization data (Figure 5) were fitted with the modified Curie−Weiss law $\chi(T) = \chi_0 + C/(T - \theta_p)$,[34] which resulted in $\chi_0 = 5.9 \times 10^{-4}$ emu/mol and $\theta_p = -8.4$ K (α-Sm_3Ge_5) and $\chi_0 = 9.3 \times 10^{-4}$ emu/mol and $\theta_p = -9.9$ K (β-Sm_3Ge_5). The corresponding Néel temperatures (T_N) were determined from the midpoint of the jump in $d\chi/dT$ and were

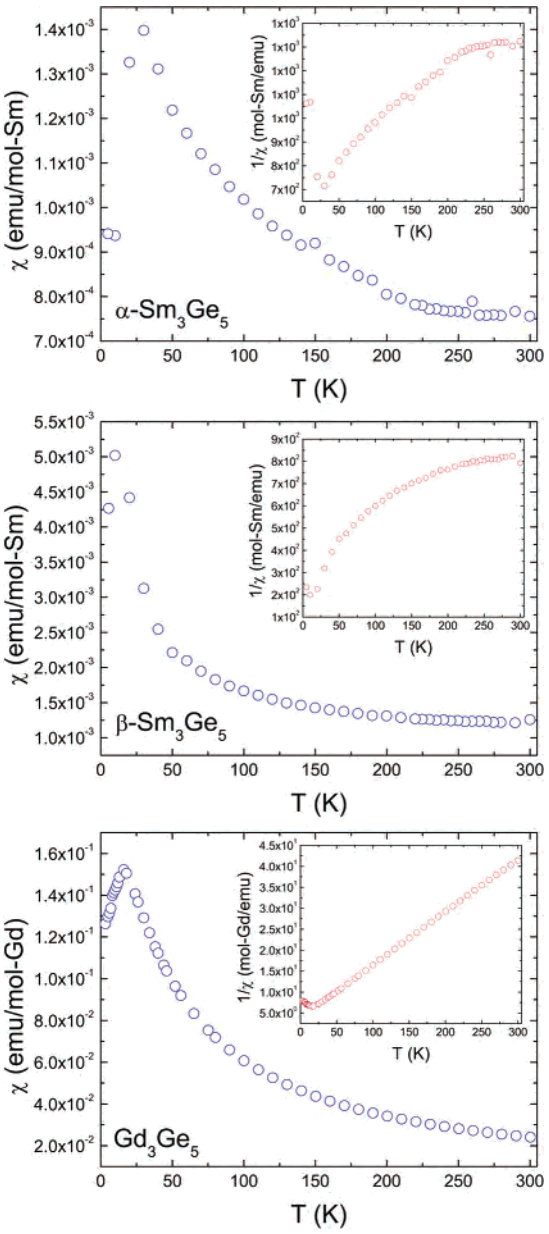

Figure 5. Magnetic susceptibility $\chi(T)$ plots for α-Sm_3Ge_5, β-Sm_3Ge_5, and Gd_3Ge_5 in a magnetic field of 500 Oe. Inverse magnetic susceptibility $\chi^{-1}(T)$ plots are shown in insets.

(32) Another polymorph of Y_3Ge_5 with the same space group as that of α-Sm_3Ge_5 has been reported but structurally not fully characterized: Venturini, G.; Ijjaali, I.; Malaman, B. *J. Alloys Compd.* **1999**, *289*, 116.

(33) Salvador, J. R.; Gour, J. R.; Bilc, D.; Mahanti, S. D.; Kanatzidis, M. G. *Inorg. Chem.* **2004**, *43*, 1403.

(34) (a) Smart, J. S. *Effective Theories of Magnetism*; Saunders: Philadelphia, PA, 1966. (b) Kittel, C. *Introduction to Solid State Physics*, 7th ed.; John Wiley and Sons: Hoboken, NJ, 1996.

$T_N = 30$ K for α-Sm_3Ge_5 and $T_N = 10$ K for β-Sm_3Ge_5. The calculated effective moments $\mu_{eff} \approx 0.70-0.80\ \mu_B$ are slightly lower than expected for Sm^{3+} from the Hund's rules for the $[Xe]f^5$ configuration.[34]

As seen from Figure 5 (bottom), Gd_3Ge_5, as expected, exhibits Curie−Weiss paramagnetic behavior at temperatures above 20−25 K. The cusp-like feature in the data around 15 K indicates the onset of long-range antiferromagnetic order. A careful examination of the data below that temperature and taking the derivative of $\chi(T)$ revealed the existence of an anomaly at around 11 K, which is indicative of a consecutive magnetic transition or of a metamagnetic transition. Calorimetry measurements provide further evidence for the second magnetic order (below). Above the Néel temperatures, $\chi(T)$ follow a Curie−Weiss law $\chi(T) = C/(T - \theta_p)$, where $C = N_A\mu_{eff}^2/3k_B$ is the Curie constant, yielding effective moments of $\mu_{eff} = 8.01\ \mu_B$ per Gd^{3+} ion in Gd_3Ge_5, in good agreement with the theoretically expected value of 7.94 μ_B according to $\mu_{eff} = g[J(J+1)]^{1/2}$.[34] The Weiss temperature θ_p is negative (−40 K) as expected for an antiferromagnetically ordered phase. No difference between zero-field-cooling and field-cooling measurements was observed.

It must be noted here that the properties of the compounds $GdGe_2$ (presumed stoichiometric, i.e., defect-free α-$ThSi_2$ type) and its nonstoichiometric analogue $GdGe_{1.67}$ ($GdSi_2$ type, disordered orthorhombic distortion of the α-$ThSi_2$ type) have been previously reported.[35] Both compounds have been found to order antiferromagnetically around 28 K and around 22 K with Weiss constants of −54 K and −26 K, respectively. Evidently, increasing the concentration of Ge defects not only induces simple tetragonal-to-orthorhombic structural change but also has a subtle effect on the magnetic interactions. The discussed herein form of Gd_3Ge_5 (ordered variant of α-$ThSi_2$ type, space group *Fdd*2) in which the defect sites are ordered completely undergoes two orderings at even lower Néel temperatures. Besides Gd_3Ge_5, none of the isostructural "3−5" phases go through multiple phase transitions.[21] Carefully synthesized and characterized $CeGe_2$ exhibits two transitions—first, antiferromagnetic with Néel temperature $T_N = 7$ K and, second, ferromagnetic with Curie temperature $T_C = 4.3$ K.[13a]

The magnetic interactions in the isostructural Tb_3Ge_5, Dy_3Ge_5, and Ho_3Ge_5 are antiferromagnetic with Néel temperatures of 17, 12, and 6 K, respectively,[21] and these are in agreement with those expected from the de Gennes scale.[34,36] Another related binary phase, Y_3Ge_5, is Pauli-paramagnetic,[37] as anticipated, while the ferromagnetic material Nd_3Ge_5 orders at temperatures below 18 K.[21a]

Resistivity and calorimetry data taken on single crystals of Gd_3Ge_5, along the direction of the plate reveal metallic behavior (Figure 6a), with $\rho_{298} \approx 526\ \mu\Omega$ cm and $\rho_5 \approx 50\ \mu\Omega$ cm, respectively. No difference between the measurements upon heating and cooling was observed, suggesting

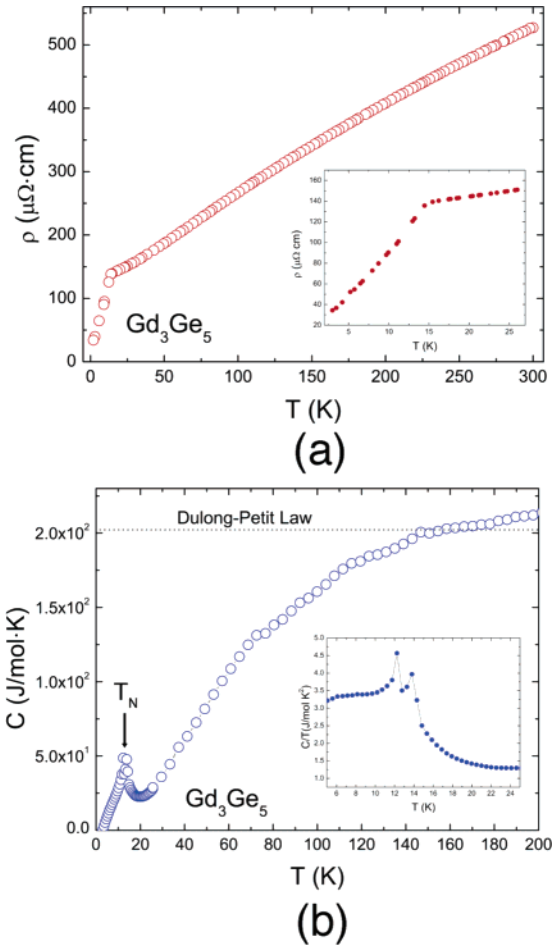

Figure 6. (a) Resistivity $\rho(T)$ and (b) heat capacity $C_p(T)$ for Gd_3Ge_5. Insets show magnified views at low temperatures.

that the charge-carrier concentration and the scattering mechanism are independent of the direction of the temperature gradient. Above ca. 20 K, the resistivity's dependence with the temperature is virtually linear, as it is expected for good metals; however, the values are more than an order of magnitude higher than the resistivities of the noble metals. The resistivity shows metallic behavior in the whole temperature range with a slight concave temperature dependence at high temperatures. At around 15 K, there is a sharp drop in $\rho(T)$ followed by a steeper and almost linear decrease with the temperature (Figure 6a, inset). This anomaly is most certainly associated with the onset of the first antiferromagnetic order, and the temperature where it occurs coincides with the Néel temperature found by measurements of the magnetic susceptibility. In the antiferromagnetic state, the electrical resistivity exhibits a T^2 temperature dependence with a T^2 resistivity coefficient of 1.6×10^{-7} [Ω cm/K^2].

The relatively high resistance at room temperature and the high residual resistivity indicate that Gd_3Ge_5 is a poor metal, in agreement with the bonding description above. Slightly lower resistivity values with similar temperature dependence have already been reported for Yb_3Ge_5 ($\rho_{298} \approx 150\ \mu\Omega$ cm, single-crystal measurements),[23] whereas the structurally unrelated Gd_5Ge_4 (also antiferromagnet with $T_N = 15$ K) exhibits low-temperature metallic and high-temperature

(35) Sekizawa, K. *J. Phys. Soc. Jpn.* **1966**, *21*, 1137.
(36) de Gennes, P. G. *J. Phys. Radium* **1962**, *23*, 510.
(37) Buschow, K. H. J.; Fast, J. F. *Phys. Status Solidi* **1967**, *21*, 593.

semiconducting behavior with a maximum in the resistivity at around 130 K $\rho_{130} \approx 22\ \mu\Omega$ cm (polycrystalline).[12]

The heat capacity of Gd_3Ge_5 as a function of the temperature is shown in Figure 6b; a well-defined peak around 15 K is clearly seen from the plot, and it confirms the onset of an antiferromagnetic order as seen from the susceptibility measurements. The specific heat asymptotically reaches a value around 210 J/mol K at high temperatures, which is in good agreement with the law of Dulong and Petit.[34] The inset of Figure 6b shows the data in the representation C_p/T versus T and provides unambiguous evidence for the second ordering transition or possible spin reorientation. However, the nature of the second transition in Gd_3Ge_5 remains unknown, and further low-temperature and field-dependent magnetization measurements are needed to fully elucidate its origin.

Conclusions

Three new binary compounds, α-Sm_3Ge_5, β-Sm_3Ge_5, and Gd_3Ge_5, have been synthesized from the corresponding elements using an excess of In to act as a metal flux. α-Sm_3Ge_5 crystallizes with a new layered hexagonal structure, which can be viewed as derivative of the AlB_2 type obtained through long-range ordering of Ge vacancies. β-Sm_3Ge_5 and Gd_3Ge_5 are new materials with the orthorhombic Y_3Ge_5 structure, which can be derived from the α-$ThSi_2$ type again through the ordering of Ge vacancies. The studies indicate that between the two Sm_3Ge_5 polymorphs α-Sm_3Ge_5 is the metastable form and β-Sm_3Ge_5 is the thermodynamically more stable phase. Temperature-dependent dc magnetization measurements show evidence of antiferromagnetic ordering below ca. 30 and 10 K for α-Sm_3Ge_5 and β-Sm_3Ge_5, respectively. Gd_3Ge_5 on the other hand undergoes two consecutive magnetic transitions below ca. 15 and 11 K. These findings are corroborated by resistivity and calorimetry measurements as well.

Exploratory syntheses using the early (La−Nd) or the late (Er−Lu) rare-earth metals show that analogous RE_3Ge_5 compounds could not be synthesized from In flux. Instead, the major products of those reactions were other binary phases whose structures are new ordered derivatives of the α-$ThSi_2$ type (La−Nd) or variants of the $ZrSi_2$ type (Er and Tm).[6] Currently, more comprehensive work in these systems is under way.

Acknowledgment. S.B. acknowledges financial support from the University of Delaware Research Foundation (UDRF) and from the University of Delaware through a start-up grant.

Supporting Information Available: A combined X-ray crystallographic file in CIF format along with plots of the crystal structures with anisotropic displacement parameters, a detailed analysis on the structure refinements using the AlB_2 and α-$ThSi_2$ models, and tables with distances. This material is available free of charge via the Internet at http://pubs.acs.org.

IC060913F